FIELD MEASUREMENTS OF ULTRASONIC STRESS IN A COMPRESSOR ROTOR

Don E. Bray
Department of Mechanical Engineering
Texas A&M University
College Station, TX 77843-3123

Wei Tang
Department of Mechanical Engineering
Texas A&M University
College Station, TX 77843-3123

Dilawar S. Grewal
Department of Mechanical Engineering
Texas A&M University
College Station, TX 77843-3123

INTRODUCTION

The run-out report for a compressor rotor showed an almost continuous bow between the two bearings, with the maximum run-out of 0.03 mm (0.0012 in)at the inlet to the fourth stage impeller. It had been run in service, and removed for normal maintenance, when the bow was observed. The seven stage compressor rotor was made of 34 Cr Ni Mo 6 steel, which is approximately a 4340 steel. It was just over 3 m in length, with diameters of approximately 265 mm at the disk mounting areas (Fig. 1). Each of the compressor stages was mounted on the rotor at the time of the stress measurement. An evaluation of the residual stress at these locations in the shaft was performed using a nondestructive technique involving critically refracted longitudinal, L_{CR}, ultrasonic waves. The L_{CR} stress measurement data showed compressive stress on the bowed side of the rotor, supporting the conclusion that residual stress is the cause of the bow. At the time that the data were taken, the rotor was horizontal, resting on two stands at the bearing ends. The following is a brief report of the test and the results. Ref. 1 should be consulted for additional detail.

Review of Progress in Quantitative Nondestructive Evaluation, Vol. 16
Edited by D.O. Thompson and D.E. Chimenti, Plenum Press, New York, 1997

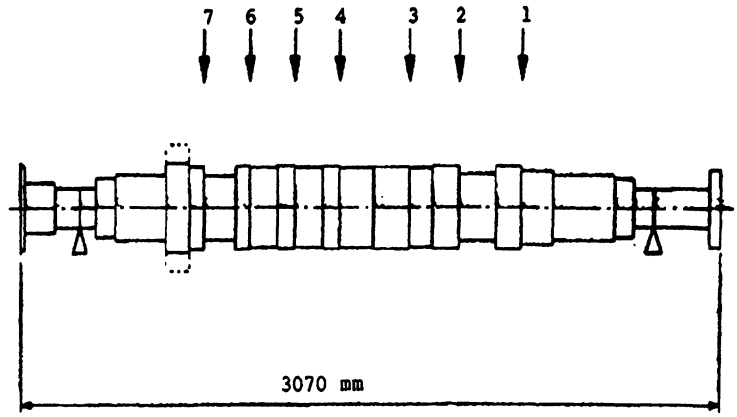

Figure 1. Rotor used for ultrasonic tests.

RESIDUAL STRESSES IN ROTORS

Normal practice is to place the surface of rotors in compression with a quenching process in manufacturing. These compressive stresses will increase the fatigue life of the rotor since they will counter tensile stresses caused by the static and dynamic forces occurring in operation. The heat treatment processes are quite complex, as described by Sholtes, Schroder and Macherauch [2] for cylinders of Ck 45 steel, an alloy steel with 0.45 C. Cylinder diameters were from 10 to 40 mm with a 100 mm length. The stresses are a result of both cooling and metallurgical transformations during the heat treatment. The cooling rate, of course, varies with depth in the cylinder, or rotor, causing differential residual stress patterns. Martensite may occur where the cooling rate is rapid, primarily at the surface and at edges. Peak axial (longitudinal) residual stresses will occur at the midpoint along the rotor length.

Residual stresses in large rotors have been investigated by Wolf and Sauer [3] using a ring core material removal method. This technique allows evaluation of residual stress at various depths in the rotors. In a rotor 3 m in length, and 1.1 m in diameter, the expected compressive stresses were found at the surface, accompanied by tensile stresses at the shaft center. Only tangential and radial stresses were measured, but axial stresses are expected to follow the pattern of the tangential stresses. At the surface, compressive tangential stresses of -12.5 to -11.5 MPa were observed. Values of -8 MPa were found at depths of approximately 20 mm. The drop off with depth was gradual, with a value of -4 MPa in the region from 40 to 80 mm deep. The stress free region was found at about 180 mm depth. The isobaric curves were quite uniform around the circular cross section of the shaft. Thus, a uniform residual stress field would be expected around the outer circumference of a typical rotor. Peak axial stresses were found at the mid-point along the length, as expected.

Placement of the disks on the rotor may result in a redistribution of the residual stresses. Uneven machined surfaces at the internal diameter of the disk and the outside diameter of the rotor can further complicate the stress patterns in the rotor.

THE L_{CR} TECHNIQUE

The L_{CR}, or the critically refracted longitudinal, wave is an acoustic wave that is excited when the angle of incidence is slightly greater than the first critical angle. It is a bulk longitudinal wave, traveling just below the surface of the specimen. This wave, however, is particularly sensitive to stress fields in a finite thickness and not just at the surface. Another important characteristic of this wave is that it is more sensitive to stress and, yet, less sensitive to localized material texture changes [4,5].

A typical L_{CR} wave probe system is shown in Fig. 2. The probes are arranged in a tandem fashion, with one probe acting as the transmitter and the other acting as a receiver. Distance between the probes is kept constant by physical means. Travel distance (d) was approximately 57 mm. Assuming that material variation is minimal, i.e. the shaft is homogenous, any change in travel-time (t) for the L_{CR} wave at different locations around the shaft circumference can be attributed to the presence of residual stresses. Additional details on the angle beam L_{CR} probes and beam profiles are given by Junghans and Bray [6].

The relationship of measured L_{CR} wave travel-time change and the corresponding uniaxial stress is given by Egle and Bray [7] as:

$$\Delta\sigma = \frac{E}{Lt_0}\left(t - t_0 - \Delta t_T\right) \tag{1}$$

where t is the measured travel-time, t_o is the stress-free travel time, Δt_T is the temperature effect, $\Delta\sigma$ is change in stress, E is Young's modulus, and L is the acoustoelastic constant for longitudinal waves propagating in the direction of the applied stress field. For uniform test conditions, temperature variations can be ignored.

CALIBRATION AND TEST SETUP

In order to effectively use L_{CR} waves for measurement of residual stress in a component, careful selections must be made regarding equipment, and data collection processes. The primary areas of concern are the equipment and systematic errors.

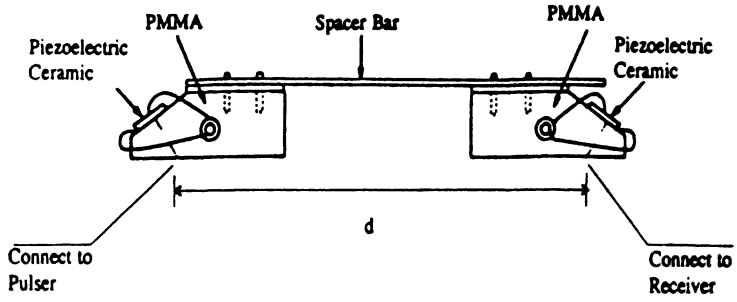

Figure 2. L_{CR} tandem probe.

Figure 3. The instruments, probes and calibration sample.

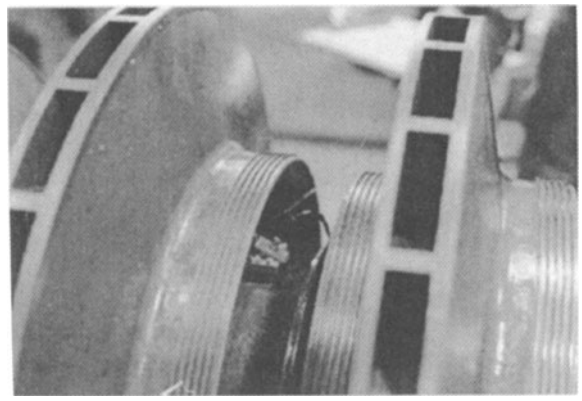

Figure 4. Probe in the place on the rotor

The equipment used in this case included the following:

LeCroy Model 9314AC Oscilloscope:		4 Channel / 400Mhz
Panametrics 5800PR Pulser/Receiver:		
Staveley ABM-0208 Probes	:	2.25MHz, 0.500"X0.500" mounted on a specially designed L_{CR} wedge.

Systematic error was reduced by maintaining a constant coupling pressure between the probe and the sample. Since the expected deviation in travel-time of the L_{CR} waves around the rotor may be less than 10 ns, it is essential that instrumentation error be limited to less than 5 ns. A calibration test specimen, similar to the rotor in shape, size and material, was constructed to evaluate the ultrasonic probe and instrumentation for deviations in a known stress free environment. The deviation in the test data on this model specimen was observed to be approximately 2 ns between locations around the calibration specimen.

ON-SITE TESTING

The calibration specimen, probes and instrumentation were transported to the shop where the rotor was stored. The instrumentation, probes and calibration sample are shown in Fig. 3. The shaft was marked circumferentially every 45° on the rotor between impellers 3 and 4, 4 and 5, and 5 and 6 from the inlet side. Fig. 4 shows the probe in place on the rotor. Data on the calibration specimen and the shaft were collected on two different instances. For every position, multiple data points were taken to constitute a single data-set for a particular location.

To further minimize the effect of experimental error, data were taken using different test plans. The first set of data were taken by keeping the probe set on the top and rotating the rotor for each test location. Other variations included keeping the shaft stationary and moving the probes around the shaft to the each location. Also, the sender and receiver probes were switched by 180° for one data set.

RESULTS

Travel-times were collected with the L_{CR} probe oriented axially (longitudinally) on the shaft, and placed at locations 0° through 315° around the shaft. Data were collected at the inlet positions to the fourth, fifth and sixth impellers. Since the variations were expected to be most pronounced at the inlet to the fourth stage, only those data are reported here. Ref. 1 contains more complete results.

Travel-time data for the inlet to the fourth stage were obtained by first collecting six different sets of travel-time profiles around the shaft. Average travel-time variations, rather than actual travel-times, are given in Table 1. The values shown are derived from the travel-times to better represent the variations around the shaft. Within each data set, the mean travel-time was established, and the variation from the mean was calculated for each location. Finally, for each location, the travel-time variations from the mean were averaged across the columns (by rows), from each of the six data sets. This presentation allowed for minimization of random signal variations and, therefore, revealed more clearly the actual variations in travel-time caused by the shaft.

Table 1: Travel-time variations (μs) and relative stress on the rotor at the inlet to the fourth stage

Location (deg)	Average (μs)	Stand. error	Stress (MPa)	Stress (ksi)
0	0.001945833	0.00096	16.17	2.343
45	-0.000270833	0.00072	-2.25	-0.326
90	0.0040875	0.00055	33.96	4.923
135	0.002495833	0.00108	20.74	3.00
180	-0.001554167	0.00078	-12.91	-1.871
225	-0.001145833	0.00078	-9.52	-1.380
270	-0.0020875	0.00089	-17.34	-2.513
315	0.0022375	0.00078	18.59	2.694
360	0.001945833	0.00096	16.17	2.343

Stress variations are estimated using Eq. 1 with assumed values for the acoustoelastic constant for the material, Young's modulus, and the appropriate travel-times. For this material, the acoustoelastic constant value we used is 2.45, which is the same as for pearlitic steel. The stress variations shown in the last column are plotted in the radar plot of Fig. 5.

SUMMARY

Critically refracted longitudinal, L_{CR}, waves were successfully employed for a comparative analysis of residual stresses at locations around the shaft of the inlet to the

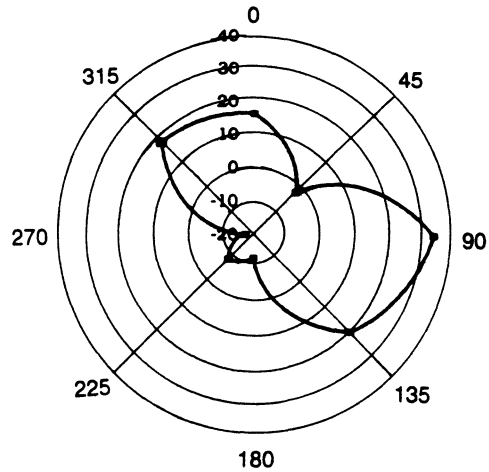

Figure 5. Stress variations (in MPa) around the rotor at the inlet to stage 4.

fourth stage of a turbine compressor rotor. Assuming that, for the most part, the shaft material is homogenous in nature, results show a stress differential of approximately 55 MPa (8 ksi) from the 90° and 135° location to the opposite 270° location on the rotor. These observed variations around the circumference of the rotor were considerably greater that those cited earlier from the results of Wolf and Sauer [2]. Significantly, the data obtained in these tests indicate a compressive stress field in the half of the rotor from 135° to 315°, compared to the other half. Results from the run-out report showed the maximum bow to be at 180°, which is certainly within the range of the compressive field indicated by the ultrasonic data. Considering other factors which affect run-out, this agreement is supportive of the ultrasonic results. Travel-time data for the fifth and sixth stages positions on the rotor were not as uniform as that found at the stage four position. No temperature variation adjustments were made to the data since the temperature variations were minimal.

REFERENCES

1. D. E. Bray, W. Tang, and D. Grewal, "Ultrasonic Stress Evaluation in a Compressor Rotor," Accepted for publication, J. of Test and Eval.
2. B. Scholtes, R. Schroder, and E. Macherauch, "Experimental and Theoretical Analysis of Internal Stresses in Quenched Steel Cylinders," *Residual Stresses,* E. Macherauch and V. Hauk, Eds., Proceedings of the European Conference on Residual Stresses, 1983. Karlsruhe, DCM Informationsgesellschaft, Verlag, Adenaueralle 21, D-6370 Oberursel 1, Germany (1986), pp. 113-124.
3. H. Wolf, and D. Sauer, "New Experimental Techniques to determine Residual Stresses in Large Turbine Components," Proceedings of the American Power Conference, Vol. 36, (1974), pp. 500 - 510.
4. D. M. Egle and D. E. Bray, "Measurement of Acoustoelastic and Third-Order Elastic Constants for Rail Steel" J. of the Acou. Soc. of Amer., Vol. 60, No. 3 (1976) pp. 741-744.
5. D. E. Bray, and R. K. Stanley, *Nondestructive Evaluation Engineering*, McGraw-Hill, New York (1989).
6. P. G. Junghans, and D. E. Bray, "Beam Characteristics of High Angle Longitudinal Wave Probes" NDE: Applications, Advanced Methods and Codes and Standards, Eds. R. N. Pangborn *et al.*, PVP-Vol. 216, NDE Vol. 9, Proceedings of the 1991 Pressure Vessels and Piping Conference, San Diego, CA, June 23-27, 1991, The American Society of Mechanical Engineers, New York, NY (1991) pp. 39-44.
7. D. E Bray,. and T. Leon-Salamanca, "Zero-Force Travel-Time Parameters For Ultrasonic Head-Waves in Railroad Rail" Materials Evaluation, Vol. 43, No. 7 (1985) pp. 854-858, 863.